ECMWF COPERNICUS REPORT

Copernicus Climate Change Service

Product Quality Assessment Report (PQAR) – ANNEX E for IASI CO_2 (v10.1) and CH_4 (v10.2) and AIRS CO_2 (v3.0) mid-tropospheric products

C3S2_312a_Lot2_DLR – Atmosphere

Issued by: C. Crevoisier, LMD/CNRS, France

Date: 14/02/2024

Ref: C3S2_312a_ Lot2_D-WP2_PQAR-2023-GHG_ANNEX-E_v7.2

Official reference number service contract: 2021/C3S2_312a_Lot2_DLR/SC1

Contributors

INSTITUTE OF ENVIRONMENTAL PHYSICS (IUP), UNIVERSITY OF BREMEN, BREMEN, GERMANY
(IUP)
M. Buchwitz

CENTRE NATIONAL DE LA RECHERCHE SCIENTIFIQUE (CNRS), LABORATOIRE DE METEOROLOGIE DYNAMIQUE (LMD), PALAISEAU, FRANCE
(LMD/CNRS)
C. Crevoisier
N. Meilhac

History of modifications

Version	Date	Description of modification	Chapters / Sections
1.1	20-October-2017	New document for data set CDR1 (until 2016)	All
2.0	4-October-2018	Update for CDR2 (until 2017)	All
3.0	12-August-2019	Update for CDR3 (until 2018) and additional information of Metop-C	All, esp. Sects. 1.1 and 2.1
3.1	03-November-2019	Update after review by Assimila: Correction of typos and broken links. Some references added.	All
4.0 beta	18-August-2020	Update for CDR4 (until 2019) with new version of each IASI product	All
4.0	17-September-2020	Correction of issues with numbering of tables and figures based on review by Assimila	All
5.0	18-February-2021	Update for CDR5 (until 2020)	All
6.0	4-August-2022	Update for CDR6 (until 2021)	All
6.1	14-December-2022	Update after review (use of new template, several improvements at various places)	All
6.2	14-February-2023	Update after 2nd review (several improvements at various places)	All
6.3	02-March-2023	Minor updates after 2nd review to generate clean version.	All
7.0	24-August-2023	Update for CDR7 (until end of 2022)	All
7.1	19-September-2023	Update after review	All
7.2(beta 1)	17-November-2023	Minor improvements after review	All
7.2 (beta 2)	1-February-2024	Improved Figs. 3, 4, 11.	Sects. 2.1 and 2.2
7.2	14-February-2024	Improved Fig. 11 and related text	Sect. 2.2.1.1

List of datasets covered by this document

Deliverable ID	Product title	Product type (CDR, ICDR)	Version number	Delivery date
WP2-FDDP-GHG-v2	CO2_IASA_NLIS	CDR 7	10.1 (CO_2)	31-Aug-2023
	CH4_IASA_NLIS	CDR 7	10.2 (CH_4)	31-Aug-2023
	CO2_IASB_NLIS	CDR 7	10.1 (CO_2)	31-Aug-2023
	CH4_IASB_NLIS	CDR 7	10.2 (CH_4)	31-Aug-2023
	CO2_IASC_NLIS	CDR 7	10.1 (CO_2)	31-Aug-2023
	CH4_IASC_NLIS	CDR 7	10.2 (CH_4)	31-Aug-2023

Related documents

Reference ID	Document
D1	**Main PQAR:** Buchwitz, M., et al., Product Quality Assessment Report (PQAR) – Main document for Greenhouse Gas (GHG: CO_2 & CH_4) data set CDR 7 (2003-2022), project C3S2_312a_Lot2_DLR – Atmosphere, 2023. *(this document is an ANNEX to the Main PQAR)*
D2	Crevoisier, C., et al., Algorithm Theoretical Basis Document (ATBD) – ANNEX E for IASI CO_2 and CH_4 and AIRS CO_2 mid-tropospheric products, project C3S2_312a_Lot2_DLR – Atmosphere, 2023.

Acronyms

Acronym	Definition
AIRS	Atmospheric Infrared Sounder
AMSU	Advanced Microwave Sounding Unit
ATBD	Algorithm Theoretical Basis Document
BESD	Bremen optimal EStimation DOAS
CAR	Climate Assessment Report
C3S	Copernicus Climate Change Service
CCDAS	Carbon Cycle Data Assimilation System
CCI	Climate Change Initiative
CDR	Climate Data Record
CDS	(Copernicus) Climate Data Store
CMUG	Climate Modelling User Group (of ESA's CCI)
CoMet	Carbon Dioxide and Methane Mission
CONTRAIL	Comprehensive Observation Network for Trace gases by Airlines
CRG	Climate Research Group
D/B	Data base
DOAS	Differential Optical Absorption Spectroscopy
EC	European Commission
ECMWF	European Centre for Medium Range Weather Forecasting
ECV	Essential Climate Variable
EMMA	Ensemble Median Algorithm
ENVISAT	Environmental Satellite (of ESA)
EO	Earth Observation
ESA	European Space Agency
EU	European Union
EUMETSAT	European Organisation for the Exploitation of Meteorological Satellites
FCDR	Fundamental Climate Data Record
FoM	Figure of Merit
FP	Full Physics retrieval method
FTIR	Fourier Transform InfraRed
FTS	Fourier Transform Spectrometer
GCOS	Global Climate Observing System
GEO	Group on Earth Observation
GEOSS	Global Earth Observation System of Systems
GHG	GreenHouse Gas
GOME	Global Ozone Monitoring Experiment
GMES	Global Monitoring for Environment and Security
HIPPO	HIAPER Pole-to-Pole Observations

GOSAT	Greenhouse Gases Observing Satellite
IAGOS	In-service Aircraft for a Global Observing System
IASI	Infrared Atmospheric Sounding Interferometer
ICOS	Integrated Carbon Observation System
IMAP-DOAS (or IMAP)	Iterative Maximum A posteriori DOAS
IPCC	International Panel in Climate Change
IUP	Institute of Environmental Physics (IUP) of the University of Bremen, Germany
JAXA	Japan Aerospace Exploration Agency
JCGM	Joint Committee for Guides in Metrology
L1	Level 1
L2	Level 2
L3	Level 3
L4	Level 4
LMD	Laboratoire de Météorologie Dynamique
MACC	Monitoring Atmospheric Composition and Climate, EU GMES project
NA	Not applicable
NASA	National Aeronautics and Space Administration
NetCDF	Network Common Data Format
NDACC	Network for the Detection of Atmospheric Composition Change
NIES	National Institute for Environmental Studies
NIR	Near Infra Red
NLIS	LMD/CNRS *neuronal* network mid/upper tropospheric CO2 and CH4 retrieval algorithm
NOAA	National Oceanic and Atmospheric Administration
Obs4MIPs	Observations for Climate Model Intercomparisons
OCO	Orbiting Carbon Observatory
OE	Optimal Estimation
PBL	Planetary Boundary Layer
ppb	Parts per billion
ppm	Parts per million
PR	(light path) PRoxy retrieval method
PVIR	Product Validation and Intercomparison Report
QA	Quality Assurance
QC	Quality Control
REQ	Requirement
RMS	Root-Mean-Square
RTM	Radiative transfer model
SCIAMACHY	SCanning Imaging Absorption spectroMeter for Atmospheric ChartographY
SCIATRAN	SCIAMACHY radiative transfer model
SRON	SRON Netherlands Institute for Space Research
SWIR	Short Wava Infra Red

TANSO	Thermal And Near infrared Sensor for carbon Observation
TANSO-FTS	Fourier Transform Spectrometer on GOSAT
TBC	To be confirmed
TBD	To be defined / to be determined
TCCON	Total Carbon Column Observing Network
TIR	Thermal Infra Red
TR	Target Requirements
TRD	Target Requirements Document
WFM-DOAS (or WFMD)	Weighting Function Modified DOAS
UoL	University of Leicester, United Kingdom
URD	User Requirements Document
WMO	World Meteorological Organization
Y2Y	Year-to-year (bias variability)

General definitions

Essential climate variable (ECV)

An ECV is a physical, chemical, or biological variable or a group of linked variables that critically contributes to the characterization of Earth's climate.

Climate data record (CDR)

The US National Research Council (NRC) defines a CDR as a time series of measurements of sufficient length, consistency, and continuity to determine climate variability and change.

Fundamental climate data record (FCDR)

A fundamental climate data record (FCDR) is a CDR of calibrated and quality-controlled data designed to allow the generation of homogeneous products that are accurate and stable enough for climate monitoring.

Thematic climate data record (TCDR)

A thematic climate data record (TCDR) is a long time series of an essential climate variable (ECV).

Intermediate climate data record (ICDR)

An intermediate climate data record (ICDR) is a TCDR which undergoes regular and consistent updates, for example because it is being generated by a satellite sensor in operation.

Satellite data processing levels

The NASA Earth Observing System (EOS) distinguishes six processing levels of satellite data, ranging from Level 0 (L0) to Level 4 (L4) as follows.

L0	Unprocessed instrument data
L1A	Unprocessed instrument data alongside ancillary information
L1B	Data processed to sensor units (geo-located calibrated spectral radiance and solar irradiance)
L2	Derived geophysical variables (e.g., XCO_2) over one orbit
L3	Geophysical variables averaged in time and mapped on a global longitude/latitude horizontal grid
L4	Model output derived by assimilation of observations, or variables derived from multiple measurements (or both)

Additional definitions as relevant for this document:

In the following some relevant Target Requirement (TR) related definitions are given. For details please see TRD (D4), 2017, ESA-CCI-GHG-URDv2.1 and CMUG-RBD, 2010:

Systematic error: component of measurement error that in replicate measurements remains constant or varies in a predictable manner

Note: "Systematic error" = "Absolute systematic error" (in contrast to "Relative systematic error" defined below).

For satellite GHG ECV products especially the "Relative systematic error" is important. The definition as used here is as follows:

Relative systematic error: Identical with "Systematic error" but after bias correction and without considering a possible "global offset" (overall mean bias). Reflects the importance of spatially and temporally correlated errors ("spatio-temporal biases"). Computed from standard deviations of spatial and temporal biases.

Bias: estimate of a systematic measurement error (JCGM, 2008).

Precision is the measure of reproducibility or repeatability of the measurement without reference to an international standard so that precision is a measure of the random and not the systematic error. Suitable averaging of the random error can improve the precision of the measurement but does not establish the systematic error of the observation (CMUG-RBD, 2010).

Note: Precision (as explained in TRD (D4)) is quantified with the standard deviation (1-sigma) of the error distribution.

Stability is a term often invoked with respect to long-term records when no absolute standard is available to quantitatively establish the systematic error - the bias defining the time-dependent (or instrument-dependent) difference between the observed quantity and the true value (CMUG-RBD, 2010).

Note: Stability requirements cover inter-annual error changes. If the change in the average bias from one year to another is larger than the defined values, the corresponding product does not meet the stability requirement.

Representativity is important when comparing with or assimilating in models. Measurements are typically averaged over different horizontal and vertical scales compared to model fields. If the measurements are smaller scale than the model it is important. The sampling strategy can also affect this term (CMUG-RBD, 2010).

Threshold requirement: The threshold is the limit at which the observation becomes ineffectual and is not of use for climate-related applications (CMUG-RBD, 2010).

Goal requirement: The goal is an ideal requirement above which further improvements are not necessary (CMUG-RBD, 2010).

Breakthrough requirement: The breakthrough is an intermediate level between the "threshold" and "goal"requirements, which - if achieved - would result in a significant improvement for the targeted application. The breakthrough level may be considered as an optimum, from a cost-benefit point of view when planning or designing observing systems (CMUG-RBD, 2010).

Horizontal resolution is the area over which one value of the variable is representative of (CMUG-RBD, 2010).

Vertical resolution is the height over which one value of the variable is representative of. Only used for profile data (CMUG-RBD, 2010).

Observing Cycle (or **Revisit Time)** is the temporal frequency at which the measurements are required (CMUG-RBD, 2010).

Table of Contents

Scope of document

This document is a Product Quality Assessment Report (PQAR) for the Copernicus Climate Change Service (C3S, https://climate.copernicus.eu/) greenhouse gas (GHG) component as covered by project C3S2_312a_Lot2.

Within this project satellite-derived atmospheric carbon dioxide (CO_2) and methane (CH_4) Essential Climate Variable (ECV) data products will be generated and delivered to ECMWF for inclusion into the Copernicus Climate Data Store (CDS) from which users can access these data products and the corresponding documentation.

The satellite-derived GHG data products are:

- Column-averaged dry-air mixing ratios (mole fractions) of CO_2 and CH_4, denoted XCO_2 (in parts per million, ppm) and XCH_4 (in parts per billion, ppb), respectively.
- Mid/upper tropospheric mixing ratios of CO_2 (in ppm) and CH_4 (in ppb).

This document describes the validation / quality assessment of the C3S products CO2_IASA_NLIS (v10.1), CH4_IASA_NLIS (v10.2), CO2_IASB_NLIS (v10.1), CH4_IASB_NLIS (v10.2), CO2_IASC_NLIS (v10.1), CH4_IASC_NLIS (v10.2), CO2_AIRS_NLIS (v3.0).

These products are mid-tropospheric CO_2 and CH_4 Level 2 products as retrieved from the IASI sensors on Metop-A, Metop-B and Metop-C and mid-tropospheric CO_2 from AIRS using algorithms developed at CNRS-LMD, France.

Executive summary

This document describes the performance for the Level 2 CO_2 and CH_4 data products retrieved from IASI observations at CNRS-LMD and delivered to the Copernicus Climate Change Service (C3S). These products are mid-tropospheric-averaged dry-air mixing ratios (mole fractions) of CH_4 and CO_2, retrieved at 9:30 am/pm (local time) from observations made by the IASI and AMSU instruments onboard the European Metop-A (July 2006-August 2021), Metop-B (since February 2013) and Metop-C (since May 2019) platforms, and mid-tropospheric-averaged dry-air mixing ratios (mole fractions) of CO_2, retrieved at 13:30 am/pm (local time) from observations made by the AIRS and AMSU instruments onboard NASA Aqua platform.

IASI and AIRS observations were spatially and temporally collocated with observations made from aircraft measurements from the CONTRAIL (Machida et al., 2007, 2008; Matsueda et al., 2008; Sawa et al., 2015) and HIPPO (Wofsy et al. 2012**)** programs, as well as with observations made from balloons using AirCores (Membrive et al., 2017). When enough in-situ data were available, a number of statistics, including accuracy and stability, have been computed from the difference between in-situ measurements and retrievals from space observation. Overall, the CNRS-LMD products are found to be highly stable and meet the Target Requirements (TR) for accuracy and stability. It should be noted that, due to too sparse a validation dataset for CH_4, the TR for stability could not be computed. This calls for continuous effort in performing and developing continuous airborne observations of greenhouse gases.

1. Product validation methodology

1.1 CH_4 and CO_2 mid-tropospheric column averaged mole fractions

The validation is performed for five Level 2 products:

- CO2_IASA_NLIS: mid-tropospheric column averaged mole fractions of CO_2 retrieved from IASI onboard Metop-A.
- CO2_IASB_NLIS: mid-tropospheric column averaged mole fractions of CO_2 retrieved from IASI onboard Metop-B.
- CO2_IASC_NLIS: mid-tropospheric column averaged mole fractions of CO_2 retrieved from IASI onboard Metop-C.
- CH4_IASA_NLIS: mid-tropospheric column averaged mole fractions of CH_4 retrieved from IASI onboard Metop-A.
- CH4_IASB_NLIS: mid-tropospheric column averaged mole fractions of CH_4 retrieved from IASI onboard Metop-B.
- CH4_IASC_NLIS: mid-tropospheric column averaged mole fractions of CH_4 retrieved from IASI onboard Metop-C.
- CO2_AIRS_NLIS: mid-tropospheric column averaged mole fractions of CO_2 retrieved from AIRS onboard Aqua.

As described in [D2], the six first products have been retrieved from simultaneous observations of the IASI and AMSU instruments flying together onboard the Metop satellites using a non-linear inference scheme based on neural networks. IASI hyperspectral observations in the thermal infrared at 7.7 µm for CH_4 or 15 µm for CO_2, which are sensitive to both temperature and gas concentrations of CH_4 or CO_2, respectively, are used in conjunction with microwave observations from the AMSU instruments, only sensitive to temperature, to decorrelate both signals (Crevoisier et al., 2009a, 2009b, 2013). The fifth product has been similarly obtained with AIRS and AMSU observations.

Potential radiative systematic biases existing between simulations used in the inference scheme and observations are computed for each channel by averaging, over the instruments full years of operation, the differences between simulations and collocated (in time and space) satellite observations. The simulations are performed using the 4A/OP-2009 forward model[1] (*Scott and Chédin, 1981*), which is based on the updated 2011 version of the GEISA spectroscopic database[2] (Jacquinet-Husson et al., 2011), and radiosonde measurements from the Analyzed Radio Soundings Archive database[3] IASI calibrated radiance spectra (level1c) are received through the EUMETCast near real time data distribution service via the French AERIS center[4].

[1] Available at https://4aop.aeris-data.fr, last access August 2023

[2] Available at https://geisa.aeris-data.fr/, last access August 2023

[3] Available at http://ara.lmd.polytechnique.fr, last access August 2023

[4] https://www.aeris-data.fr/, last access August 2023

The retrieved CO_2 and CH_4 integrated columns are weighted to the tropical mid-troposphere with peak sensitivity at about 230 hPa (~11 km), half the peak sensitivity at 100 and 500 hPa (~6 and 16 km), and no sensitivity to the surface. Retrievals are performed over land and sea, by night and day (9:30 am/pm local time) for clear-sky only (no clouds, no aerosols). The CO_2 retrievals are limited to the tropical region (30N:30S) because of the greater stability of the temperature atmospheric profile, which helps decorrelating temperature from gas in the observed radiances, yielding a much better precision compared to the extratropics.

In order to cope with failure of various AMSU channels on each Metop satellites, version 10.1 (MT-CO_2) and version 10.2 (MT-CH_4) of the retrieval has been designed to process the entire time series of Metop-A, Metop-B and Metop-C data with the same retrieval code that excludes all failed AMSU channels. This yields a homogeneous data set of mid-tropospheric CH_4 and CO_2 from the three instruments over the entire time period since the first launch of IASI onboard Metop-A.

Current versions of the retrievals (v10.1 (CO_2) and v10.2 (CH_4)) are based on the use of a single AMSU channel (#6) to cancel out the temperature signals in the IASI TIR radiances. Until 2022, this channel was available on the 3 Metop platforms enabling the use of the same inversion scheme for the 3 Metop platforms. Unfortunately, the radiometric noise of AMSU channel 6 onboard Metop-B has been increasing rapidly for the last 6 months of 2023, as seen in Figure 1. This rapid increase is impacting the CO2/CH4 products from Metop-B, yielding a rapid increase in the product standard deviations as seen in Figure 2.

Figure 1: Time series of the NEΔT of the AMSU channel 6 onboard Metop-B (provided by NOAA/NESDIS/STAR[5])

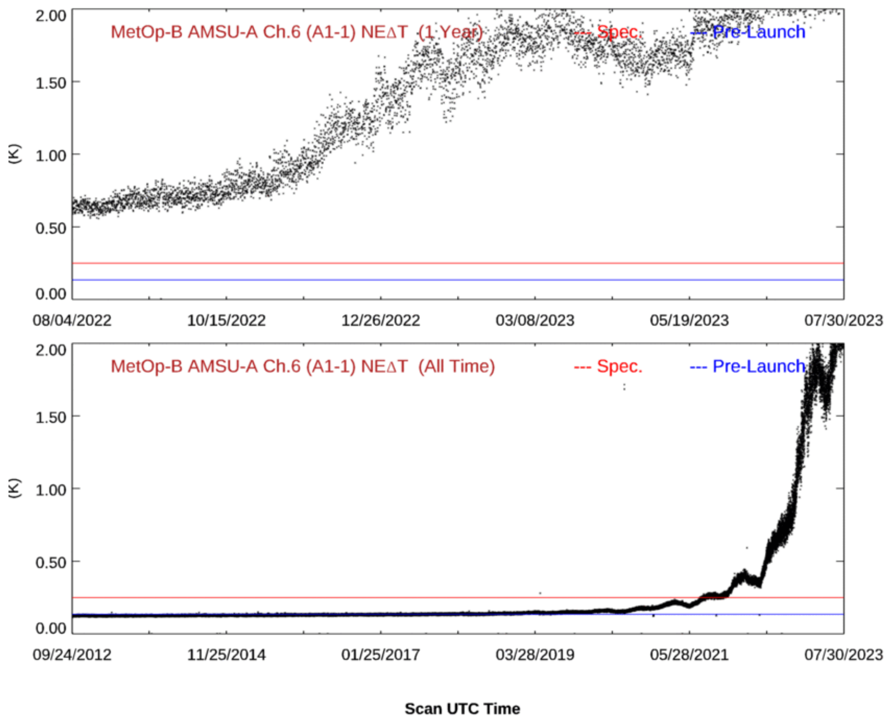

[5] https://www.star.nesdis.noaa.gov/icvs/status_MetOPB_AMSUA.php, last access August 2023

Figure 2: Time series of the mean of the 5°X5° gridded box standard deviations of MT-CH_4 v10.2 (red) and MT-CO_2 v10.1 (blue) from Metop-B since 2013.

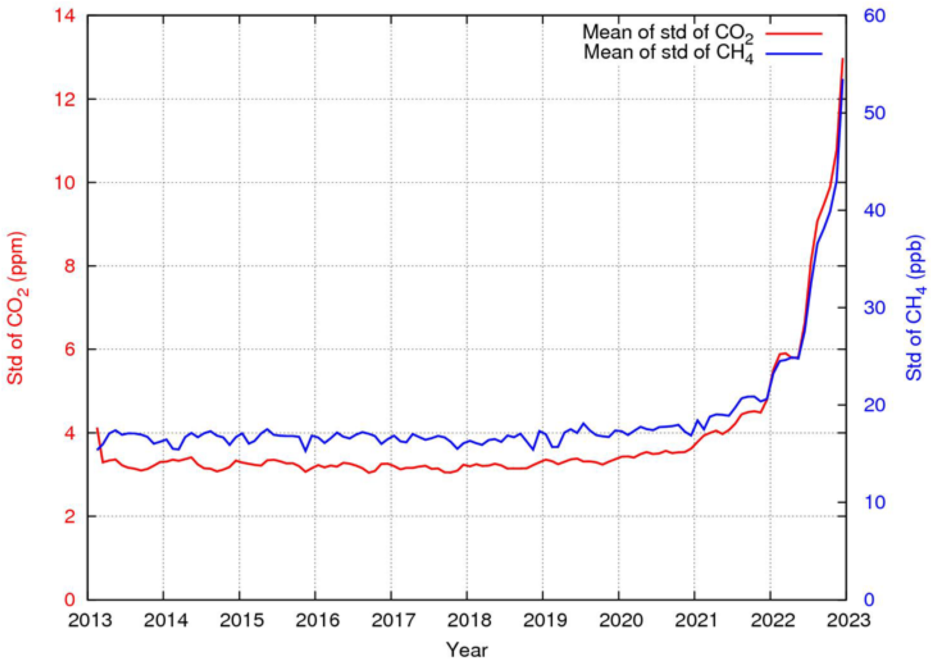

1.2 Validation data and method

Validation against high precision / low systematic errors reference observations is required for the mid/upper troposphere CO_2 and CH_4 data products. Unfortunately, measurements of both gases in the free troposphere and stratosphere are every sparse. Validation thus mostly relies on existing aircraft and airborne measurements.

A promising way consists in using 0-30 km concentration profiles measured by balloon-borne atmospheric samplers called AirCores (Karion et al., 2010; Membrive et al., 2017) to which averaging kernels can be applied to derive columns that can then be compared to those derived from space. So far, only a few profiles have been acquired, all in the northern hemisphere. In this validation exercise, use is made of CH_4 profiles from all stations operated by European teams for which data are available: three stations located in France where monthly measurements are made in the framework of the French AirCore program[6] (Aire-sur-l'Adour, Trainou, Reims), two stations also managed by the French AirCore team (Timmins, Ontario, Canada and Kiruna in Sweden). Additional profiles acquired through a cooperation with the Finnish Meteorological Institute come from Sodankylä. Spanning 2014-2019, they are used to validate both Metop-A and Metop-B retrievals (CH4_IASA_NLIS and CH4_IASB_NLIS).

[6] https://aircore.aeris-data.fr, last access January 2023

Additional validation data come from measurements performed by commercial aircrafts made as part of the CONTRAIL project (Matsueda et al. 2008, Machida et al., 2008, Sawa et al., 2015). Concentration of CO_2 and CH_4 are then provided at the altitude of the flight, typically at 10-12 km for most of the flight, and as profile during ascend or descent at airports. For previous years, use is made of in situ observations made by commercial airliners from April 1993 to March 2007 between Japan and Australia[7]. These observations, partly analyzed by Matsueda et al. (2002), are available on a monthly basis. They cover the altitude range 9–13 km. Several gaps have affected the measurements throughout the period, which prevents making robust statistics from them.

[7] Data available at https://gaw.kishou.go.jp/

2. Validation Results

2.1 Products CO2_IASA_NLIS and CO2_IASB_NLIS

2.1.1 Validation

2.1.1.1 Validation with aircraft measurements

Figure 3 shows comparison of IASI CO_2 mid-tropospheric columns with CONTRAIL aircraft data as monthly means in 12 latitudinal bands of 5° each. Figure 4 shows the scatter plot of IASI CO_2 vs. CONTRAIL CO_2 for the whole period. The R correlation coefficient is 0.99 for IASI-A (v10.1) and 0.97 for IASI-B (v10.1), the bias and the standard deviation of the difference between both being 1.00 ± 1.32 ppm. The bias for v10.1 is larger than for previous versions. This might come from the change in the retrieval code that has led to a change in the vertical sensitivity to CO_2 variations as explained in [D2]. With a higher sensitivity to CO_2 at lower altitudes than previous versions, the difference between the partial column retrieved from IASI and the in-situ concentration measured at 11-12 km by CONTRAIL is expected to be higher.

To compute the various parameters summarized in the following tables, the time series in each latitudinal band displayed in Figure 3 have been used separately.

Table 1 shows the mean CONTRAIL-IASI-A CO_2 difference together with the associated standard deviation recorded in each latitudinal band. The mean CONTRAIL-IASI-A bias over all latitudinal band is 1.21 ppm. It comes down to 0.75 ppm when we restrict to 25S:25N, where most of the reference data are available.

Table 1: Mean and standard deviation (std) of CO_2 (ppm): difference between CONTRAIL and IASI (v9.1) over 12 latitudinal bands of 5° each. Statistics over July 2007-December 2019.

Latitudinal band	30S: 25S	25S: 20S	20S: 15S	15S: 10S	10S: 5S	5S :EQ	EQ: 5N	5N: 10N	10N: 15N	15N: 20N	20N: 25N	25N: 30N
IASI-CONTRAIL Mean	3.69	2.17	0.79	0.00	-0.23	-0.03	0.38	0.48	0.57	1.22	2.13	3.38
IASI-CONTRAIL std	1.29	1.13	0.86	0.80	0.95	1.02	0.96	0.91	0.71	0.74	0.90	1.12

Figure 3: Monthly variation of IASI mid-tropospheric CO_2 v10.1 (dashed line) for Metop-A (upper panel) and Metop-B (lower panel) from July 2007 to September 2021 and of CONTRAIL CO_2 (full line) from July 2007 to December 2016 in 12 latitudinal bands of 5° each from 30S to 30N.

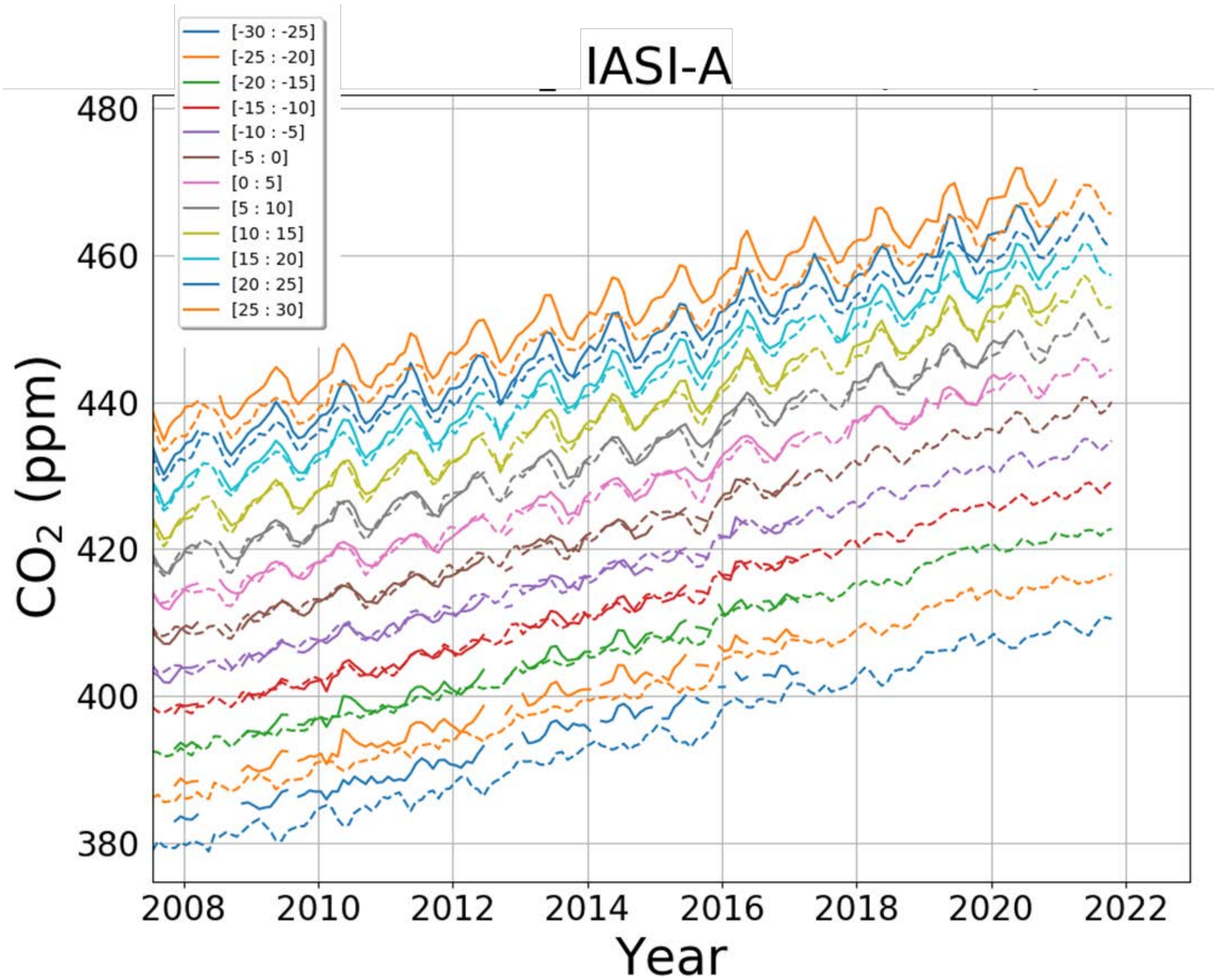

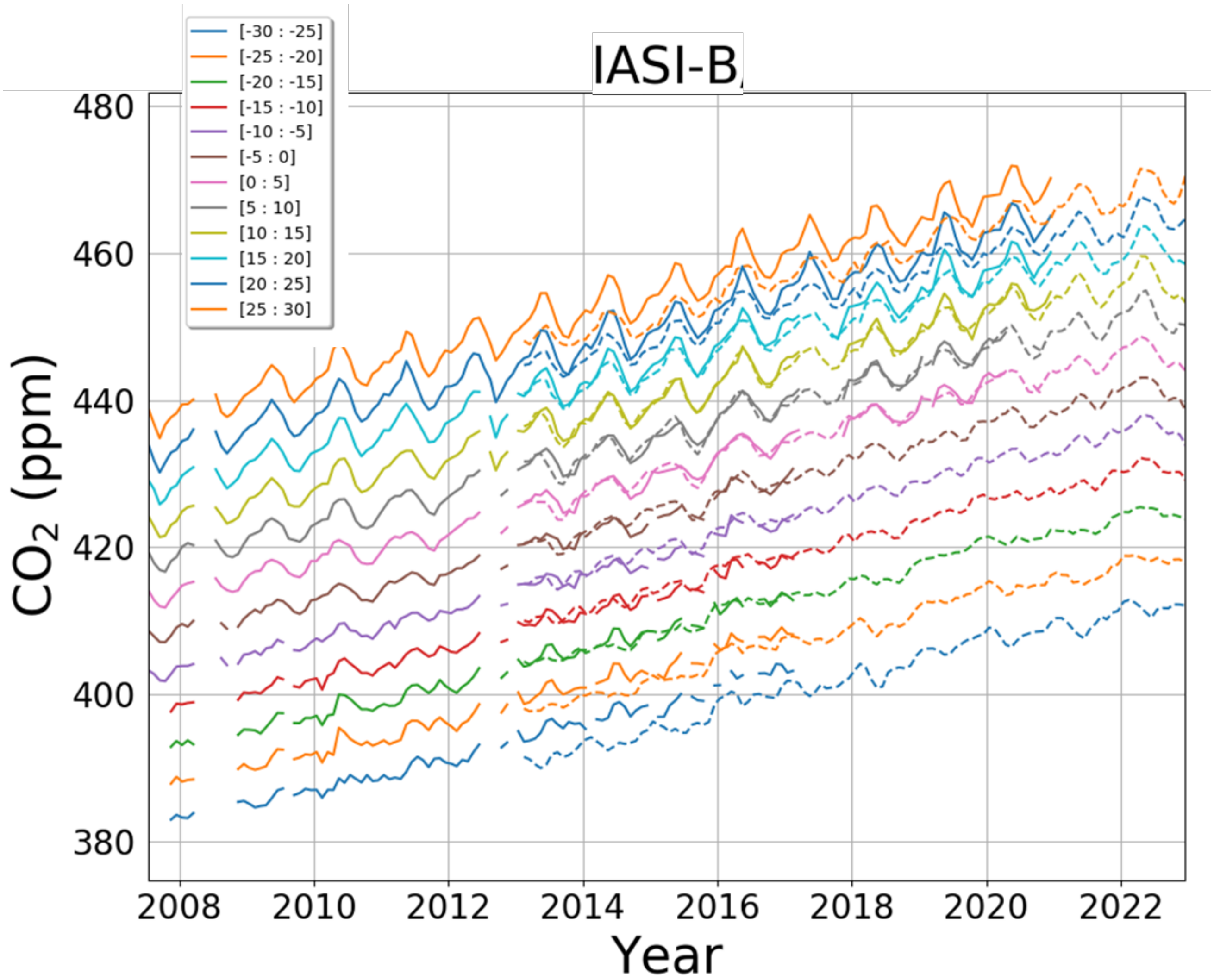
IASI-B
[-30 : -25]
[-25 : -20]
[-20 : -15]
[-15 : -10]
[-10 : -5]
[-5 : 0]
[0 : 5]
[5 : 10]
[10 : 15]
[15 : 20]
[20 : 25]
[25 : 30]
480
460
440
420
400
380
CO_2 (ppm)
2008
2010
2012
2014
2016
2018
2020
2022
Year

Figure 4: Scatter plot of IASI mid-tropospheric CO_2 v10.1 (IASI-A on left and IASI-B on right) vs. CONTRAIL CO_2 measured at 10 km over the whole period available for CONTRAIL depicted in Fig. 1 (July 2007 – December 2020) measured by aircraft at 10-12 km (dashed line) in 12 latitudinal bands of 5° each.

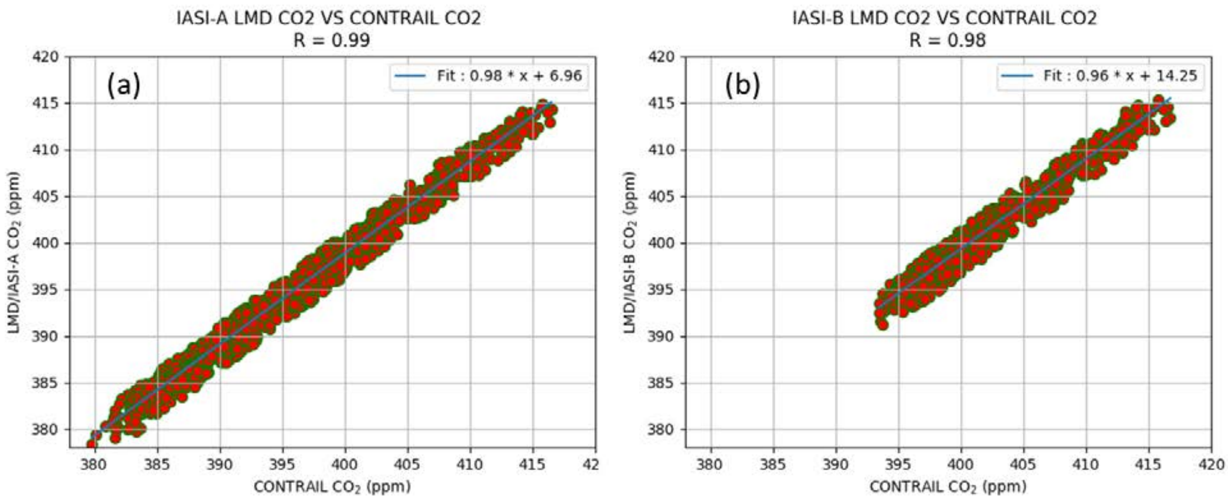

The relative systematic error is computed as the standard deviation of the CONTRAIL – IASI bias obtained in each latitudinal band. It is computed as two values:

- the “relative spatial bias”, which is the standard deviation of the mean per-latitudinal band bias computed over the entire time series. This was found to be 1.27 ppm.
- The “relative spatio-temporal bias”, which is the standard deviation of the seasonal mean bias in each latitudinal band (i.e. JFM, AMJ, JAS, OND). This was found to be 1.61 ppm.

For each latitudinal band, the linear drift was computed as the slope of the linear regression of the mean CONTRAIL –IASI bias against time. Table 2 shows the resulting drift and error. The main drift over all bands is 0.03 ± 0.06 ppm/year.

Table 2: Linear drift of CO_2 (ppm).

Latitudinal band	30S: 25S	25S: 20S	20S: 15S	15S: 10S	10S: 5S	5S :EQ	EQ: 5N	5N: 10N	10N: 15N	15N: 20N	20N: 25N	25N: 30N
Linear drift [ppm/year]	0.05	-0.06	0.01	0.00	-0.03	-0.08	0.02	0.04	0.10	0.13	0.02	0.10

Finally, the year-to-year stability in each latitudinal band was computed as the difference between the maximum and the minimum values of the monthly differences within each year. This stability was found to be 2.07 ± 0.58 ppm/year.

2.1.1.2 Consistency between Metop-A, Metop-B and Metop-C

A direct comparison between mid-tropospheric CO_2 fields retrieved from Metop-A and Metop-B (version v10.1) yields a global bias and standard deviation of -0.35 ppm +/- 0.45 ppm. Between Metop-B and Metop-C, a global bias and standard deviation is given by 0.22 ppm +/- 0.59 ppm.

Figure 5 shows the full time series of mid-tropospheric CO_2 retrieved from Metop-A, Metop-B and Metop-C. For most of the common period, the three products, which are recorded at the same local time but with a 180° shift in the orbit, are consistent with each other.

Figure 5: Mid-tropospheric CO_2 retrieved from IASI/AMSU onboard Metop-A (purple) between July 2007 and November 2020; from IASI/AMSU onboard Metop-B (green) between February 2013 and December 2022 and from IASI/AMSU onboard Metop-C (cyan) between May 2019 and December 2022.

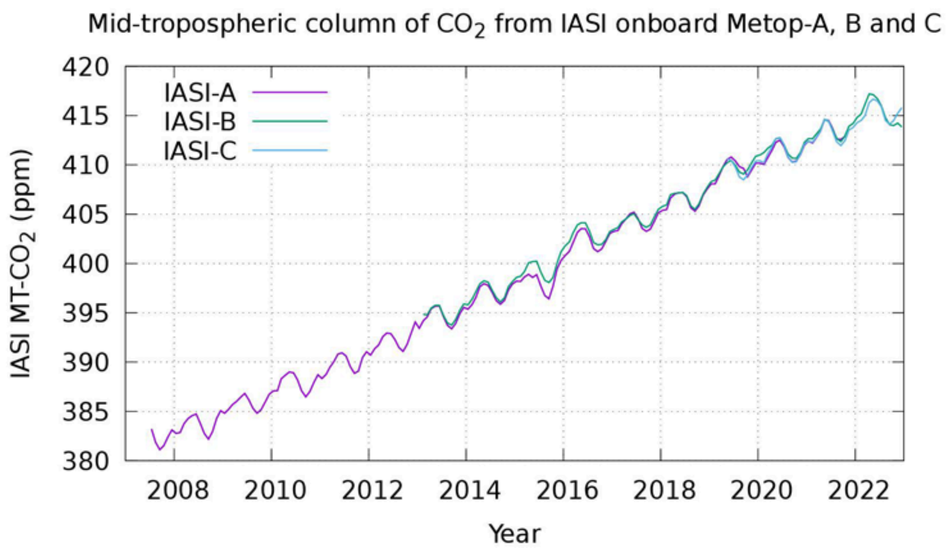

Figure 6 shows the seasonal maps (3 months average) of mid-tropospheric CO_2 retrieved from Metop-A and Metop-B. Figure 7 shows the difference between the two and the associated standard deviation, over the whole period common between the instruments (2014-2021). Figure 8 and 9 are the same as Figures 6 and 7 but for the comparison between Metop-B and Metop-C, over 2018-2022. The Metop-A, -B and -C derived fields are close to each other. However, a small but positive bias for latitudes higher than 30 degrees can be seen. These biases appear to be constant throughout the year. Such constant biases might be due to the change from a tropical air mass to a mid-latitude air mass that is not consistent between the two instruments; this point will be checked for future releases.

Figure 6: Seasonal maps (3 months average) of mid-tropospheric CO_2 as retrieved from Metop-A (left) and Metop-B (right), average over 2014-2021.

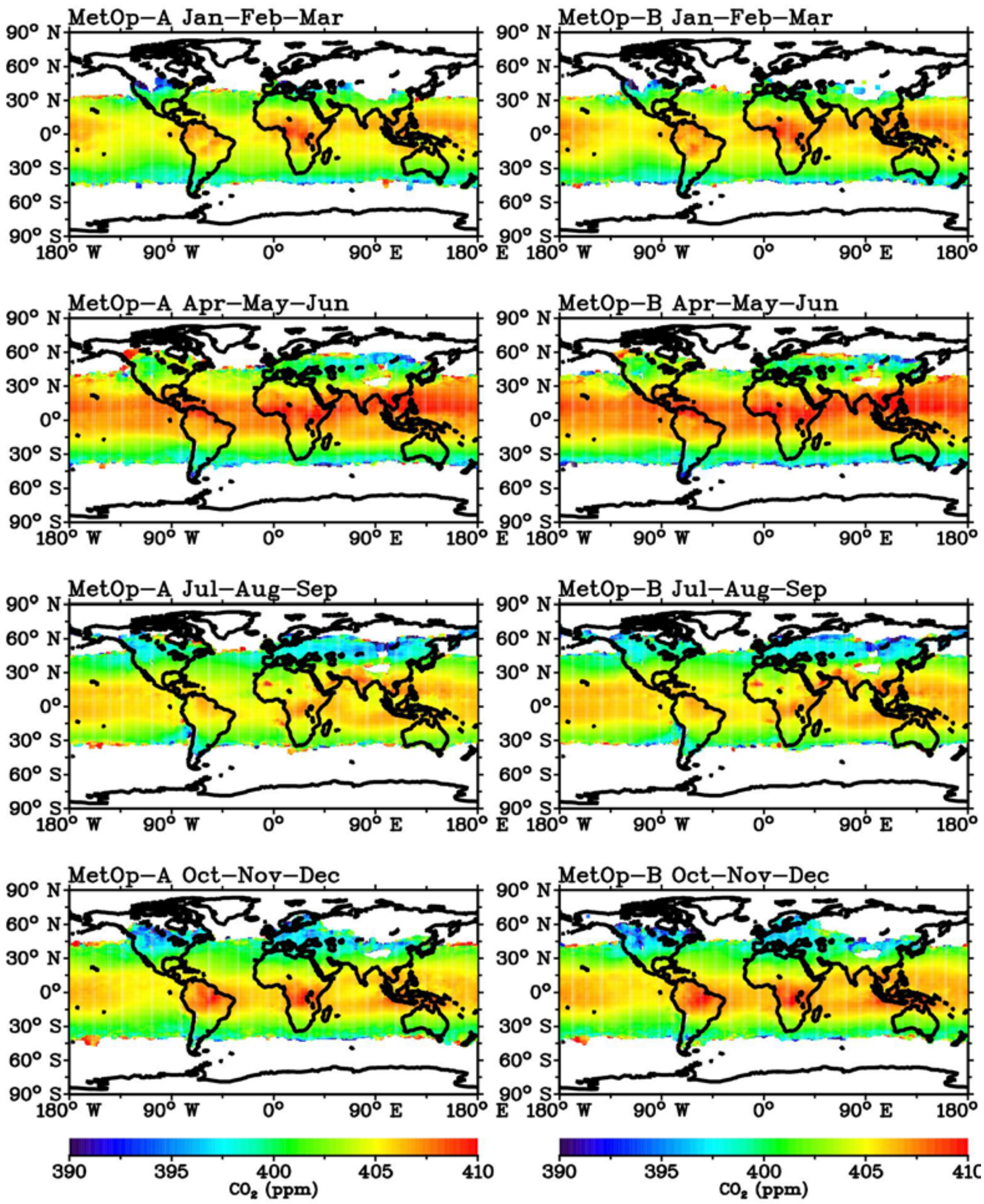

Figure 7: Seasonal maps (3 months average) of mid-tropospheric CO_2: Mean (left) and standard deviation (right) of the difference between Metop-A and Metop-B, average over 2014-2021.

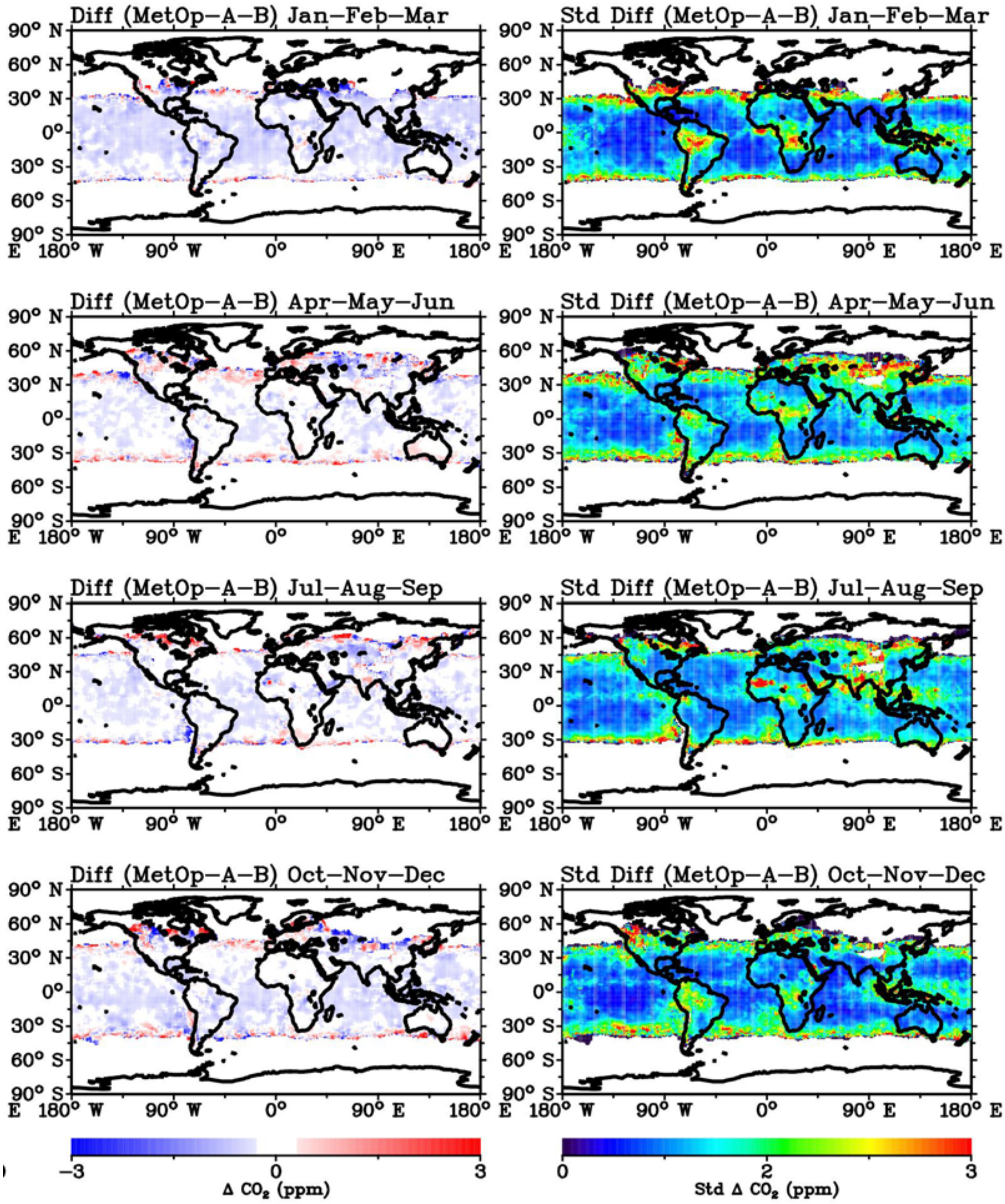

Figure 8: Seasonal maps (3 month average) of mid-tropospheric CO_2 as retrieved from Metop-B (left) and Metop-C (right), average over 2019-2022.

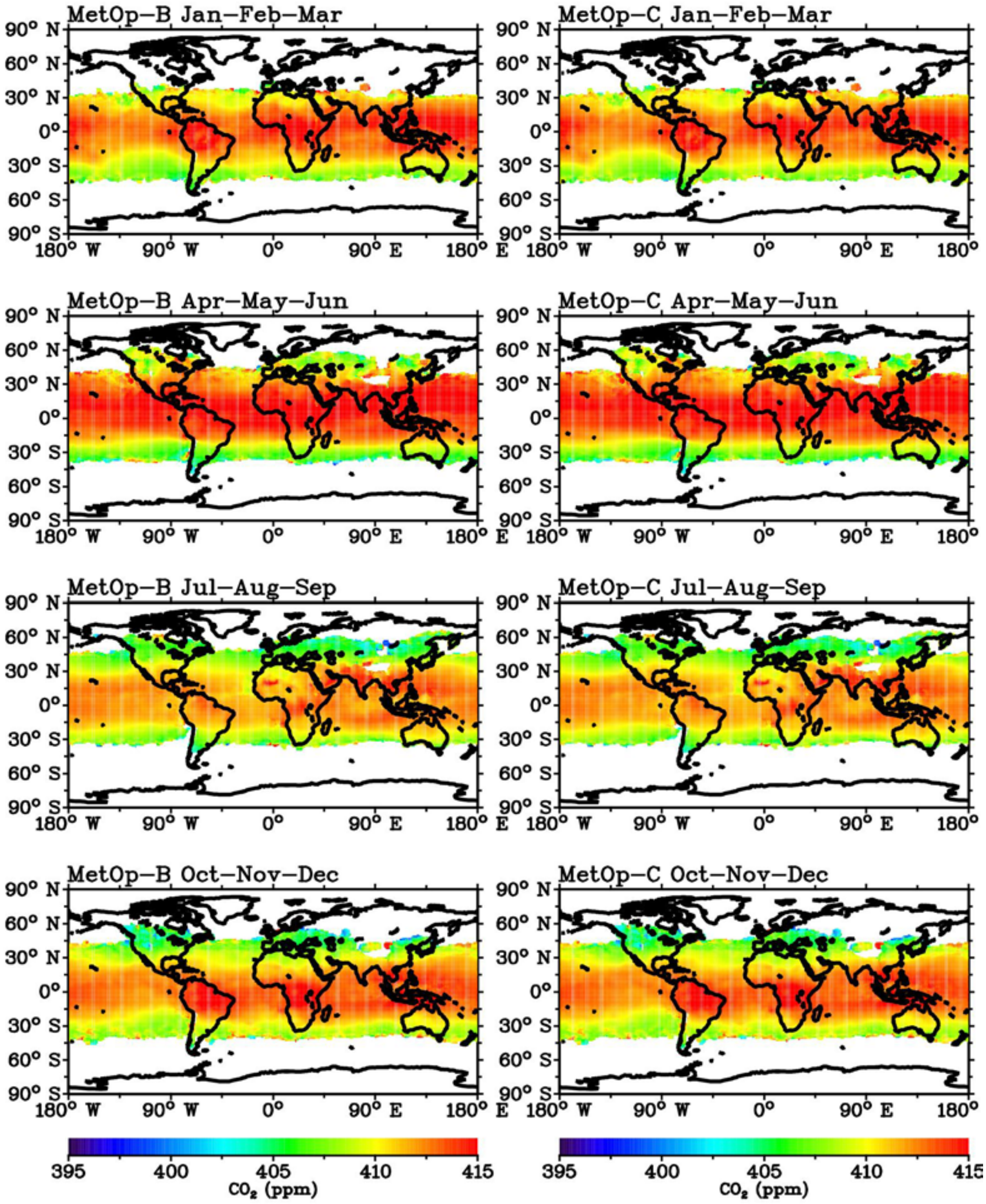

Figure 9: Seasonal maps (3 month average) of mid-tropospheric CO_2: Mean (left) and standard deviation (right) of the difference between Metop-B and Metop-C, average over 2019-2022.

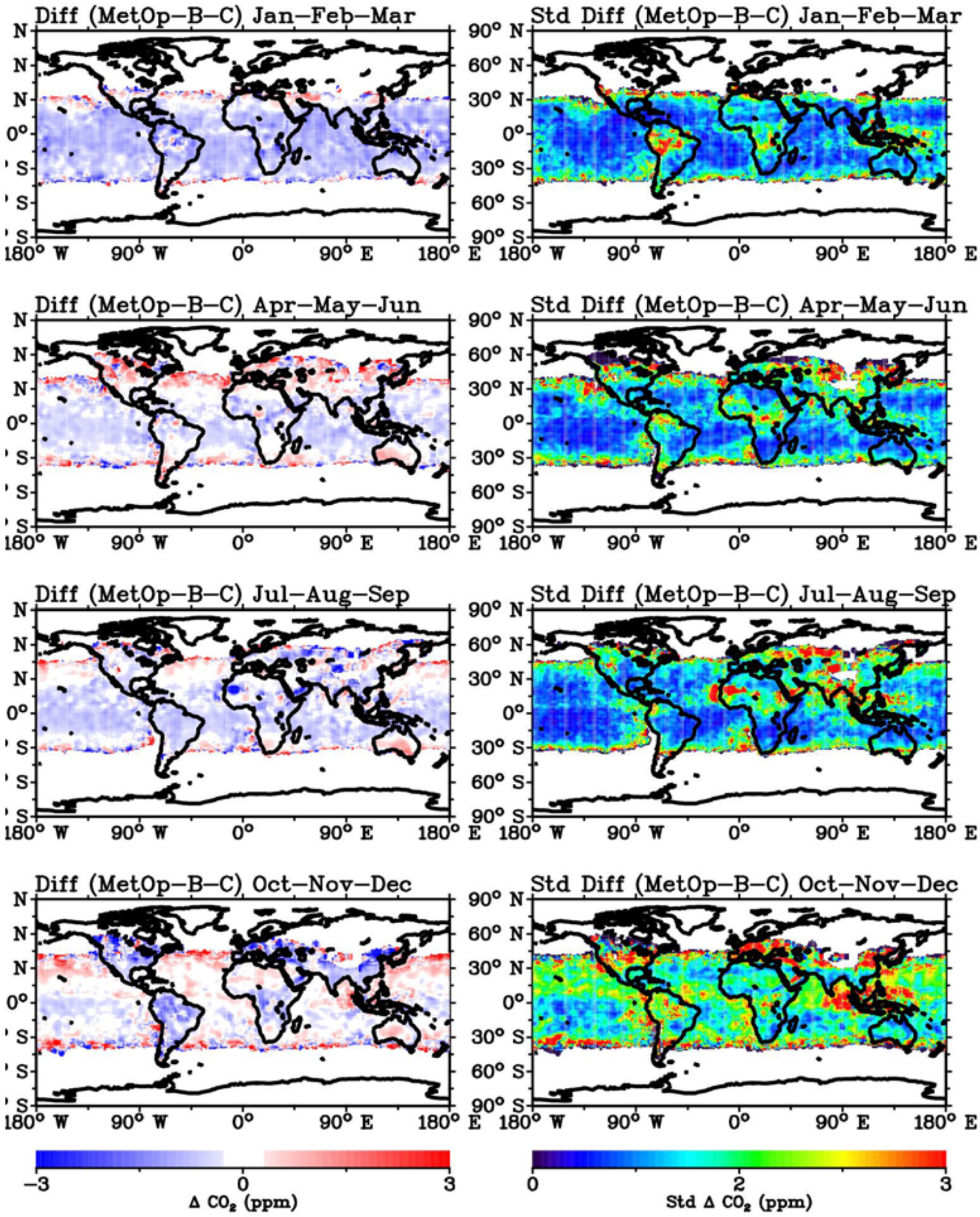

2.1.2 Validation summary

The validation results are summarized in Table 3.

Table 3: Product Quality Summary Table for product CO2_IASA_NLIS. T means Threshold; B means Breakthrough; G means Goal.

Product Quality Summary Table for Product: CO2_IASA_NLIS Level: 2, Version: 10.1, Time period covered: 7.2007 – 10.2021				
Parameter [unit]	Achieved performance	Requirement	TR	Comments
Single measurement precision (1-sigma) in [ppm]	0.99	< 8 (T) < 3 (B) < 1 (G)	-	-
Mean bias [ppm]	1.21	-	-	No requirement but value close to zero expected for a high quality data product.
Accuracy: Relative systematic error [ppm]	Spatial – spatiotemporal: 0.96 / 1.09	< 0.5	Probability that accuracy TR is met: 50%	This value is based on the comparison between partial column and point measurement.
Stability: Drift [ppm/year]	0.03 ± 0.06 (1-sigma)	< 0.5	Probability that stability TR is met: 100%	-
Stability: Year-to-year bias variability [ppm/year]	2.07 ± 0.58 (1-sigma)	< 0.5	-	-

2.2 Products CH4_IASA_NLIS and CH4_IASB_NLIS

2.2.1 Validation

For CH_4 products, only two quantities have been evaluated so far: single measurement precision, and mean bias with both aircraft and AirCore measurements. Due to limited time series of both aircraft and balloons, it has not yet been possible to evaluate the stability criteria.

2.2.1.1 Validation with aircraft measurements

Retrievals are compared with measurements made in the framework of the CONTRAIL project (*Machida et al., 2007, 2008; Matsueda et al., 2008; Sawa et al., 2015*). All IASI retrievals falling in a 5°x5° grid cell centered on each CONTRAIL measurement are averaged. Figure 10 shows the scatter plot of each pair of CONTRAIL / IASI CH_4. Over the whole dataset, the difference between CONTRAIL and IASI CH_4 are -1.35 ± 16.9 ppb for IASI-A and 0.95 ± 14.9 ppb for IASI-B, with a correlation R factor of 0.75 for IASI-A and 0.77 for IASI-B.

Figure 10: CONTRAIL CH_4 vs. IASI CH_4 (Metop-A on left and Metop-B on right) for all CONTRAIL measurements over July 2007-December 2017. The 1x1 line is shown as black.

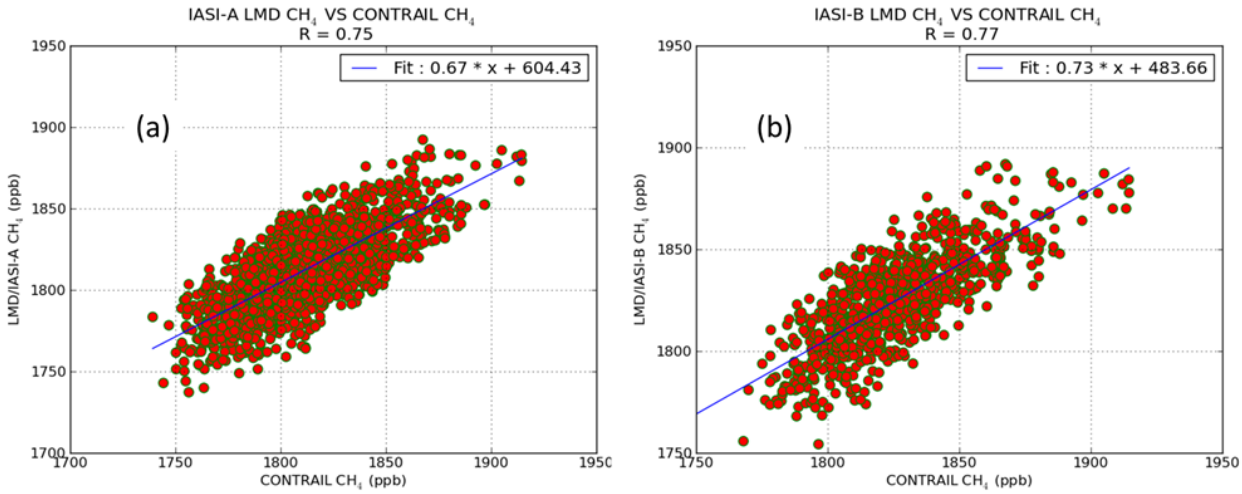

Figure 11 shows the monthly evolution of CH_4 as measured by CONTRAIL (dashed lines) and retrieved by IASI (full line) for 8 latitudinal bands of 10° each. The monthly evolution observed on both datasets is consistent whatever the latitude is, both in terms of seasonality and amplitude. Table 4 summarizes the statistics (mean and standard deviation) obtained within each 8 latitudinal bands for IASI, CONTRAIL and the difference between both. Both datasets are statistically in agreement. The standard deviations of IASI and CONTRAIL inside a given latitudinal band are noticeably close to each other.

Table 4: Mean and standard deviation of CH_4 (ppb): as measured by CONTRAIL aircrafts, as retrieved by IASI, and difference between the two over 7 latitudinal bands of 10° each. Statistics over July 2007-December 2017.

Latitudinal band	30S:40S	30S:20S	20S:10S	10S:EQ	EQ:10N	10N:20N	20N:30S	30N:40N
CONTRAIL	1812.81 ± 15.61	1799.25 ± 19.06	1798.00 ± 20.85	1800.08 ± 22.40	1813.32 ± 21.61	1825.25 ± 24.23	1831.82 ± 23.28	1833.62 ±26.07
IASI A	1811.19 ± 16.77	1797.42 ± 18.58	1799.48 ± 19.43	1802.15 ± 20.06	1819.68 ± 23.14	1826.52 ±21.33	1828.66 ±18.01	1831.59 ± 18.67
IASI-CONTRAIL	-1.62 ± 18.21	-1.83 ± 12.71	1.48 ± 11.80	2.07 ± 14.96	6.36 ± 14.62	1.27 ± 15.26	-3.16 ± 16.81	-2.03 ± 19.68

Figure 11: Comparison between CONTRAIL and IASI CH_4 over July 2007-December 2017. Monthly evolution of CONTRAIL CH_4 (dashed line) and IASI CH_4 (full line) for 8 latitudinal bands of 10° each. Each curve is shifted by 30 ppb (black arrow) to allow all curves to be displayed on the same figure.

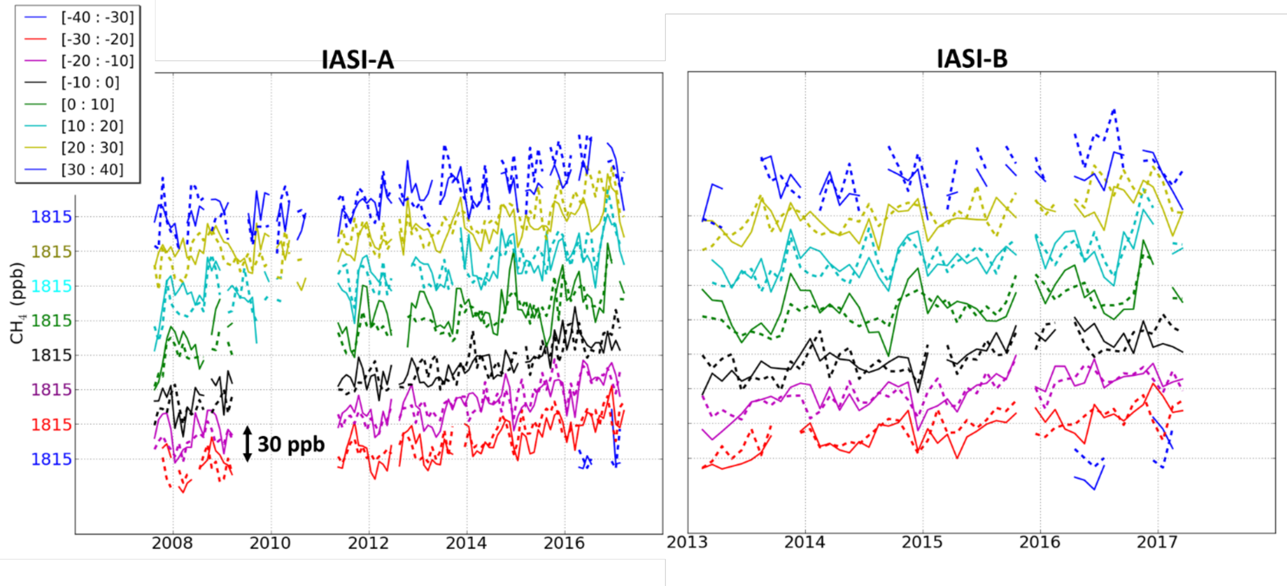

From Table 4, it is straightforward to compute the “relative spatial bias” of the “relative systematic error”, which is the standard deviation of the mean per-latitudinal band bias computed over the whole time series. The Accuracy is found to be 0.31 ppb. Due to several gaps in the time series, as can be seen in Figure 11, it is not possible to compute the “relative spatio-temporal bias” which is the standard deviation of the seasonal mean bias in each latitudinal band.

2.2.1.2 Validation with AirCore 0-30 km profiles

Here, IASI CH_4 retrievals are compared to several AirCore profiles from measurements made by the French AirCore program[8] (*Membrive et al., 2017)*. All IASI retrievals falling in a 5°x5° grid cell centered on each AirCore profile for the same day are averaged. Figure 12 shows the scatter plot of each pair of AirCore/IASI CH_4. Over the whole dataset (220 pairs for Metop-A, Metop-B and Metop-C), the difference between AirCore and IASI CH_4 is -2.9 ± 14.9 ppb.

Figure 12: Comparison between IASI CH_4 v10.2 and AirCore CH_4. Correlation is 0.64.

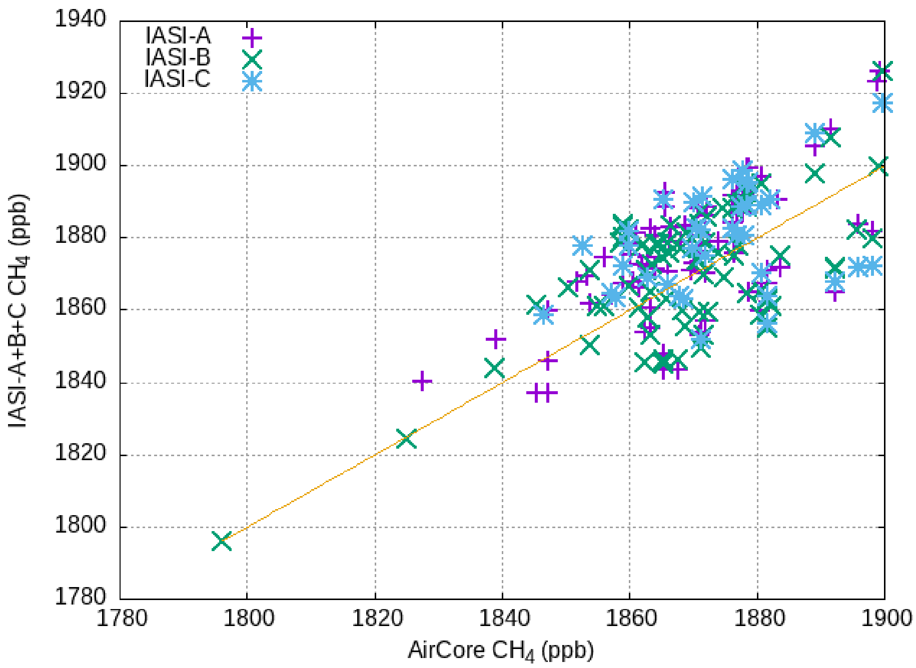

[8] https://aircore.aeris-data.fr, last access August 2023

2.2.1.3 Comparison between CH4_IASA_NLIS (Metop-A), CH4_IASB_NLIS (Metop-B) and CH4_IASC_NLIS (Metop-C)

A direct comparison between mid-tropospheric CH_4 fields retrieved from Metop-A and Metop-B (v10.2) yields a global difference of -1.36 ± 2.68 ppb and 1.23 ± 2.63 ppb. Figure 13 shows the seasonal maps (3 months average) of mid-tropospheric CH_4 retrieved from Metop-A and Metop-B. Figure 14 shows the difference between the two and the associated standard deviation, over the time period 2014-2020. Figures 15 and 16 are the same as Figures 13 and 14 but for Metop-B and C. The Metop-A and -B derived fields are close to each other. However, a small but positive bias at latitude higher than 60 degrees can be observed on the map. These biases appear to be constant throughout the year.

Figure 13: Seasonal maps (3 month average) of mid-tropospheric CH_4 as retrieved from Metop-A (left) and Metop-B (right), averaged over 2014-2021.

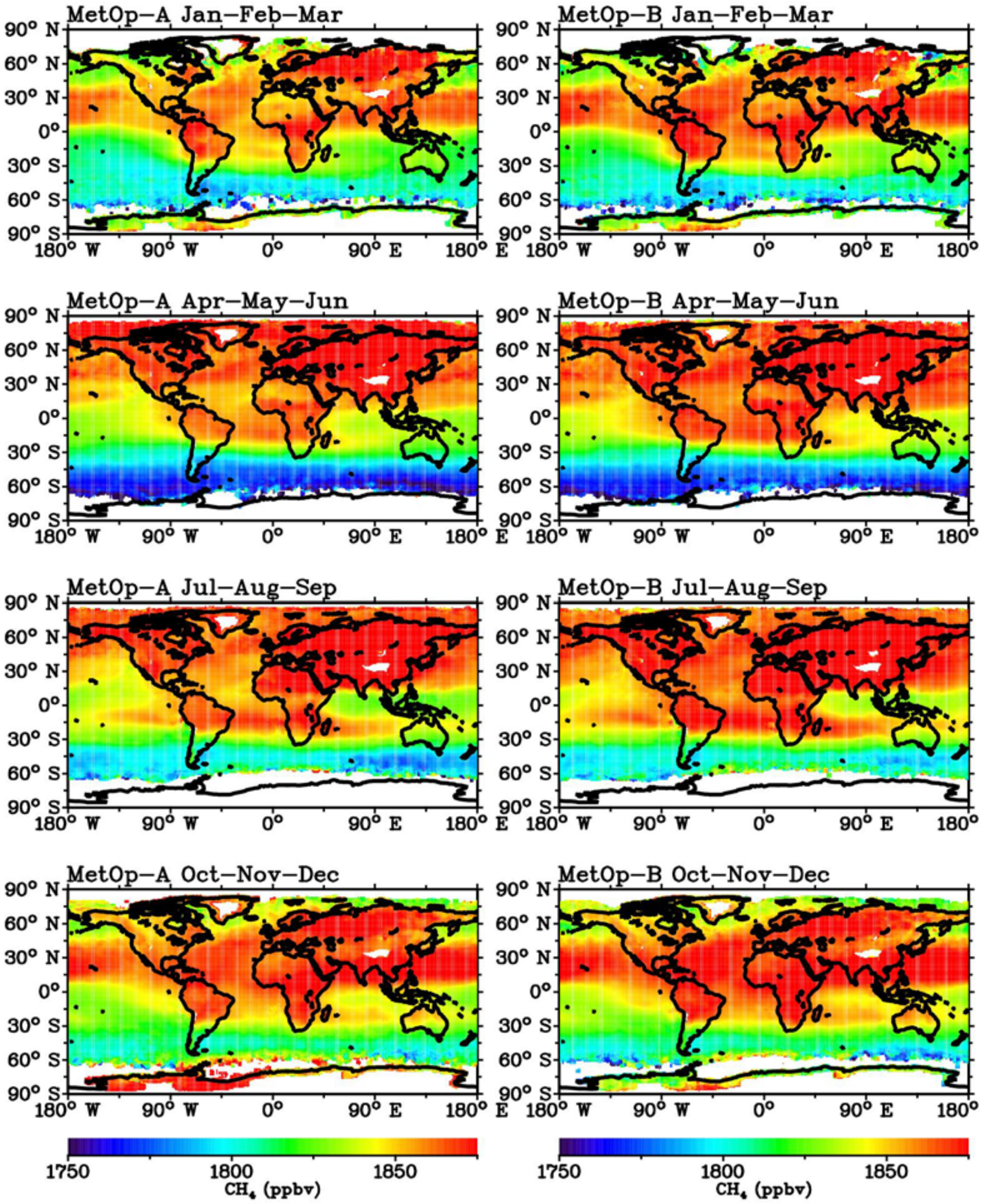

Figure 14: Seasonal maps (3 month average) of mid-tropospheric CH_4: Mean (left) and standard deviation (right) of the difference between Metop-A and Metop-B, averaged over 2014-2021.

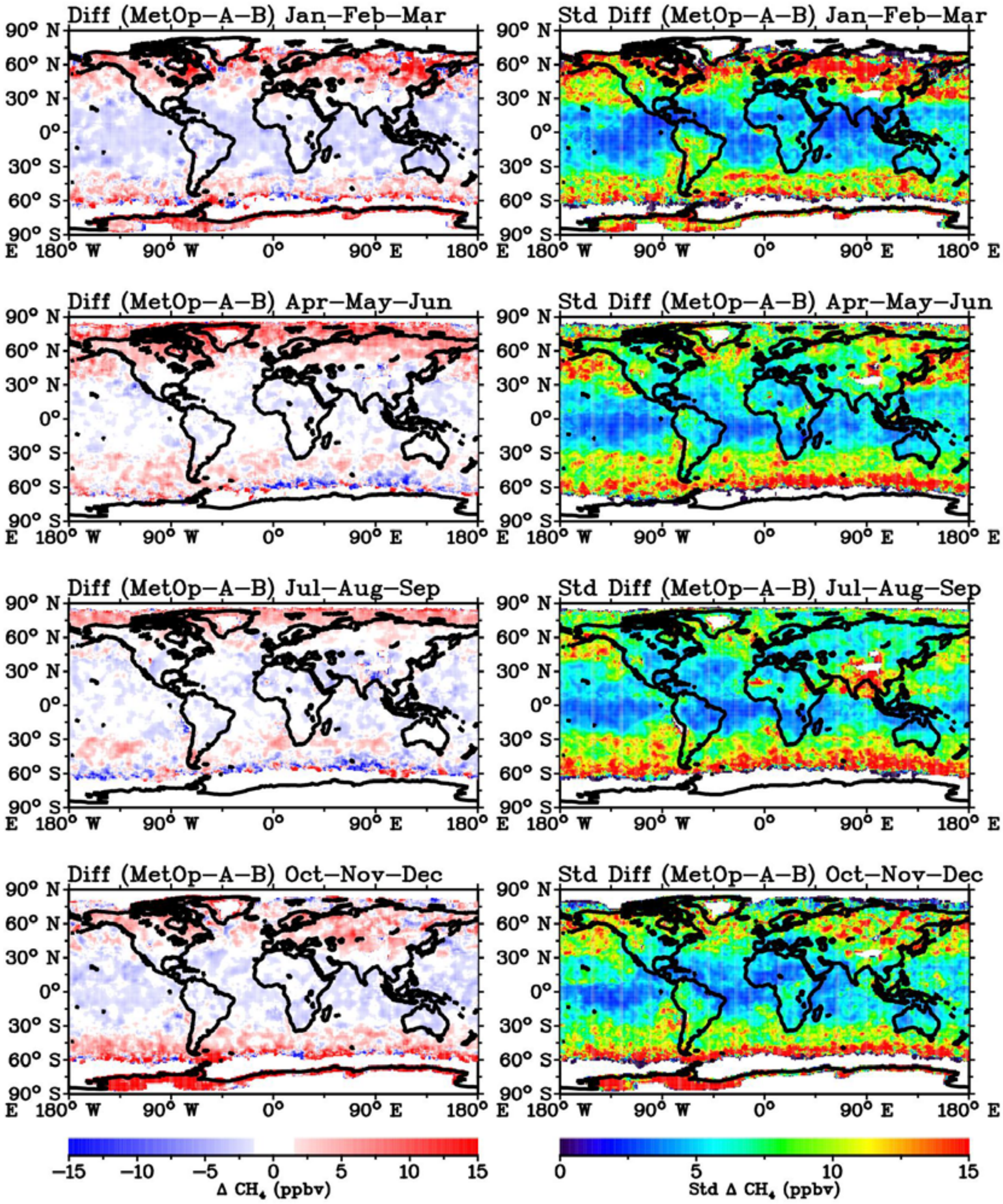

Figure 15: Seasonal maps (3 month average) of mid-tropospheric CH4 as retrieved from Metop-B (left) and Metop-C (right).

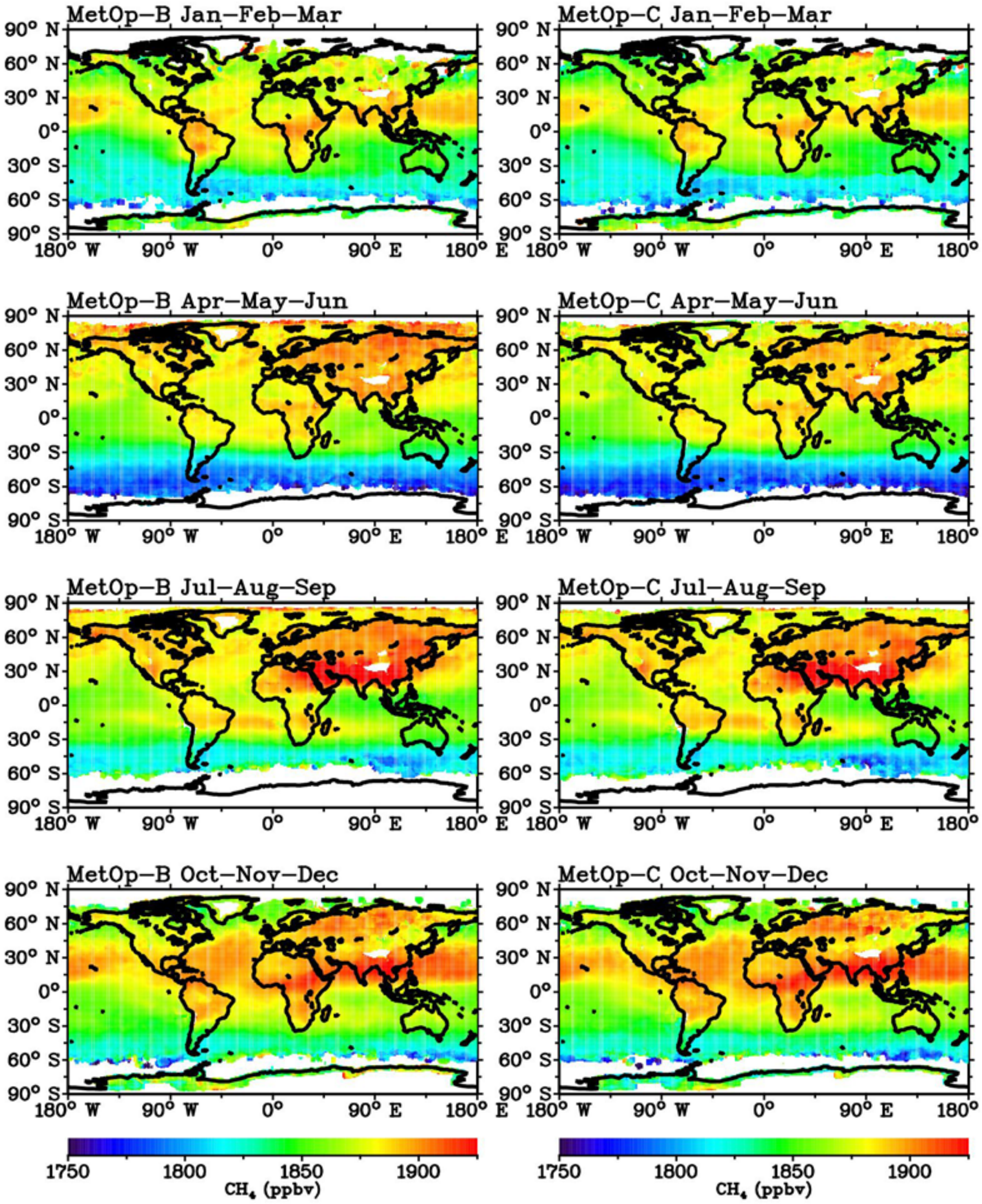

Figure 16: Seasonal maps (3 month average) of mid-tropospheric CH4: Mean (left) and standard deviation (right) of the difference between Metop-B and Metop-C.

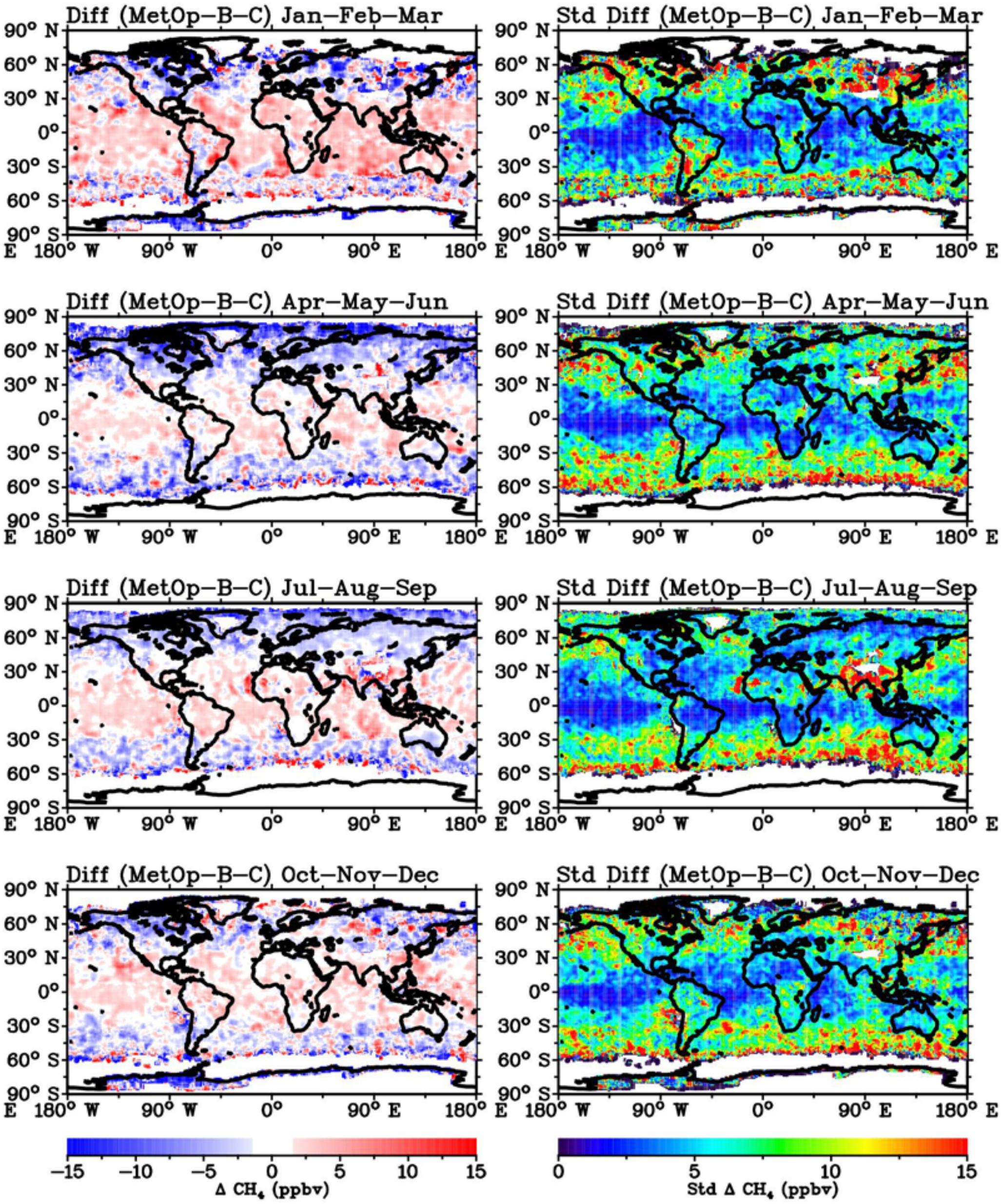

2.2.2 Validation summary

The validation results are summarized in Table 5 for CH4_IASA_NLIS. Please refer to Section 2.2.1.3 for comparison between CH4_IASA_NLIS, CH4_IASB_NLIS and CH4_IASC_NLIS.

Table 5: Product Quality Summary Table for products CH4_IASA_NLIS (NC stands for Not computed due to lack of available data). T means Threshold; B means Breakthrough; G means Goal.

Product Quality Summary Table for Product: CH4_IASA_NLIS Level: 2, Version: 10.2, Time period covered: 7.2007 – 10.2021				
Parameter [unit]	Achieved performance	Requirement	TR	Comments
Single measurement precision (1-sigma) in [ppb]	11.8	< 34 (T) < 17 (B) < 9 (G)	-	-
Mean bias [ppb]	2.93	-	-	No requirement but value close to zero expected for a high quality data product.
Accuracy: relative systematic error [ppb]	2.93	< 10	Probability that accuracy TR is met: 90%	-
Stability: Linear bias trend [ppb/year]	NC	< 3	NC	Time series of available aircraft/AirCore obs are not long enough to compute these 2 parameters
Stability: Year-to-year bias variability [ppb/year]	NC	< 3	-	

2.3 Product CO2_AIRS_NLIS

2.3.1 Validation

The seasonal cycles of CO_2 measured by JAL are plotted in Fig. 17 for the period 2005-2006 (only period with full coverage). AIRS retrieved CO_2 cycle is also plotted in Fig. 17. There is a good agreement between both datasets in terms of the phase and amplitude of the seasonal cycle. Overall, the JAL – AIRS CO_2 difference is -0.43 ± 1.32 ppm.

Beginning of mid-2006, the bias between aircraft and AIRS CO_2 increases (negative sign), up to July 2007 when AIRS channels used to perform the retrievals were lost. This might be due to a non-corrected trend, which has affected either the AMSU observations in late 2006 and 2007, or some of the AIRS channels, which started exceeding radiometric specifications.

Figure 17: Detrended CO_2 seasonal cycle in the northern tropics as measured by JAL/CONTRAIL aircraft (black) and as retrieved from AIRS (brown).

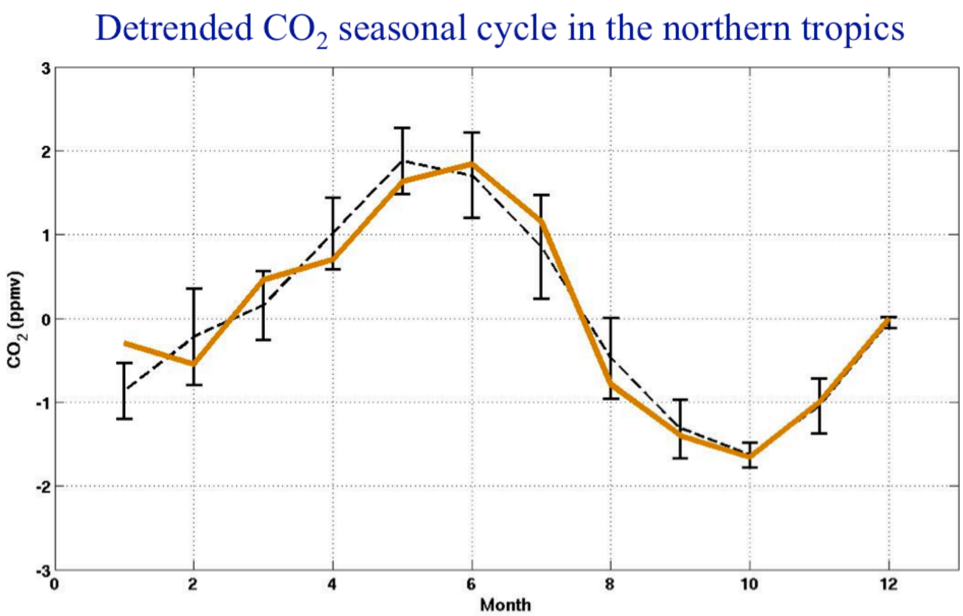

2.3.2 Validation summary

Table 6 shows the validation summary for product CO2_AIRS_NLIS.

Table 6: Product Quality Summary Table for products CO2_AIRS_NLIS. T means Threshold; B means Breakthrough; G means Goal.

Product Quality Summary Table for Product: CO2_AIRS_NLIS Level: 2, Version: 3.0, Time period covered: 4.2003 – 7.2007				
Parameter [unit]	Achieved performance	Requirement	TR	Comments
Single measurement precision (1-sigma) in [ppb]	1.32	< 8 (T) < 3 (B) < 1 (G)	-	-
Mean bias [ppb]	-0.43	-	-	No requirement but value close to zero expected for a high quality data product.

3. Application(s) specific assessments

The products can be used to monitor the evolution of major anthropogenic greenhouse gases in the atmosphere, by studying their trends, seasonality and geographical distributions (e.g., Crevoisier et al., 2013). They can also contribute to the characterization of specific emissions, such as those from rice paddies for methane or biomass burning (Thonat et al., 2015). They provide insight on global methane emissions by complementing observations of total columns of methane with observations only sensitive to the troposphere (Cressot et al., 2014).

4. Compliance with user requirements

Mid-tropospheric CO_2:

The single measurement precision of product CO2_IASA_NLIS (from IASI on Metop-A) is 1 ppm. The mean bias (global offset) is 0.96 ppm. The estimated relative accuracy is around 1 ppm. The probability that the < 0.5 ppm user requirement is met has been estimated to 50% taking into account the uncertainty of the reference data and assessment method. The product is also very stable (0.06 +/- 0.10 ppm/year (1-sigma)) meeting the requirement for long-term drift stability. The performance of product CO2_IASB_NLIS (from IASI on Metop-B) is similar.

Mid-tropospheric CH4:

The single measurement precision of product CH4_IASA_NLIS (from IASI on Metop-A) is 12 ppb. The mean bias (global offset) is -3.4 ppb. The product appears to meet the “relative systematic error” requirement of better than 10 ppb: the estimated relative accuracy is 3.4 ppb. The product appears to be very stable but a quantitative analysis could not be carried out due to lack of reference data. The performance of product CH4_IASB_NLIS (from IASI on Metop-B) is similar.

References

Buchwitz et al., 2017: ESA Climate Change Initiative (CCI) Product Validation and Intercomparison Report (PVIR) for the Essential Climate Variable (ECV) Greenhouse Gases (GHG) for data set Climate Research Data Package No. 4 (CRDP#4), Version 5.0, 9. Feb. 2017, 2017.

CMUG-RBD, 2010: Climate Modelling User Group Requirements Baseline Document, Deliverable 1.2, Number D1.2, Version 1.3, 2 Nov 2010.

Cressot et al. 2014: Cressot C., Chevallier F., Bousquet P., Crevoisier C., Dlugokencky E.J., Fortems-Cheiney A., Frankenberg C., Parker R., Pison I., Scheepmaker R.A., Montzka S.A., Krummel P.B., Steele L.P., and Langenfelds R.L., On the consistency between global and regional methane emissions inferred from SCIAMACHY, TANSO-FTS, IASI and surface measurements, Atmos. Chem. Phys., 14, 577-592 doi:10.5194/acp-14-577-2014, 2014.

Crevoisier et al., 2004: Crevoisier, C., S. Heilliette, A. Chédin, S. Serrar, R. Armante, and N. A. Scott, Midtropospheric CO_2 concentration retrieval from AIRS observations in the tropics, Geophys. Res. Lett., 31, L17106, doi:10.1029/2004GL020141, 2004.

Crevoisier et al., 2009: Crevoisier, C., Chédin, A., Matsueda, H., et al., First year of upper tropospheric integrated content of CO_2 from IASI hyperspectral infrared observations, *Atmos. Chem. Phys.*, 9, 4797-4810, 2009.

Crevoisier et al. 2009b: Crevoisier, C., Nobileau, D., Fiore, A., Armante, R., Chédin, A., and Scott, N. A.: Tropospheric methane in the tropics – first year from IASI hyperspectral infrared observations, Atmos. Chem. Phys., 9, 6337–6350, doi:10.5194/acp-9-6337-2009, 2009b.

Crevoisier et al., 2013: Crevoisier, C., Nobileau, D., Armante, R., et al., The 2007–2011 evolution of tropical methane in the mid-troposphere as seen from space by MetOp-A/IASI, *Atmos. Chem. Phys.*, 13, 4279-4289, 2013.

GCOS-154: Global Climate Observing System (GCOS): SYSTEMATIC OBSERVATION REQUIREMENTS FOR SATELLITE-BASED DATA PRODUCTS FOR CLIMATE - 2011 Update - Supplemental details to the satellite-based component of the "Implementation Plan for the Global Observing System for Climate in Support of the UNFCCC (2010 Update)", December 2011, prepared by World Meteorological Organization (WMO), Intergovernmental Oceanographic Commission, United Nations Environment Programme (UNEP), International Council for Science, Doc.: GCOS 154, 2011.

GCOS-200: The Global Observing System for Climate: Implementation Needs, World Meteorological Organization (WMO), GCOS-200 (GOOS-214), pp. 325, link: http://unfccc.int/files/science/workstreams/systematic_observation/application/pdf/gcos_ip_10oct2016.pdf, 2016.

Jacquinet-Husson et al. 2011: Jacquinet-Husson N., L. Crépeau, R. Armante, C. Boutammine, A. Chédin, et al.. The 2009 edition of the GEISA spectroscopic database, J. Quant. Spectrosc. Radiat. Transfer,112, 2395-2445 doi:10.1016/j.jqsrt.2011.06.004, 2011.

Machida et al. 2008: Machida, T., Matsueda, H., Sawa, Y., Nakagawa, Y., Hirotani, K., Kondo, N., Goto, K., Nakazawa, T., Ishikawa, K., and Ogawa, T.: Worldwide measurements of atmospheric CO_2

and other trace gas species using commercial airlines, J. Atmos. Ocean. Tech., 25(10), 1744–1754, doi:10.1175/2008JTECHA1082.1, 2008.

Matsueda et al. 2008: Matsueda, H., Machida, T., Sawa, Y., Nakagawa, Y., Hirotani, K., Ikeda, H., Kondo, N., and Goto, K.: Evaluation of atmospheric CO_2 measurements from new flask air sampling of JAL airliner observation, Pap. Meteorol. Geophys., 59, 1–17, 2008.

Membrive et al. 2017: Membrive, O., Crevoisier, C., Sweeney, C., Danis, F., Hertzog, A., Engel, A., Bönisch, H., and Picon, L.: AirCore-HR: a high-resolution column sampling to enhance the vertical description of CH_4 and CO_2, Atmos. Meas. Tech., 10, 2163-2181, https://doi.org/10.5194/amt-10-2163-2017, 2017.

Sawa et al. 2015: Sawa, Y., Machida, T., Matsueda, H., Niwa, Y., Tsuboi, K., Murayama, S., Morimoto, S., and Aoki, S.: Seasonal changes of CO_2, CH_4, N_2O, and SF_6 in the upper troposphere/lower stratosphere over the Eurasian continent observed by commercial airliner, Geophys. Res. Lett., 42, 2001–2008, https://doi.org/10.1002/2014GL062734, 2015.

Scott and Chédin 1981: Scott N.A. and Chédin A., A fast line-by-line method for atmospheric absorption computations: The Automatized Atmospheric Absorption Atlas, J. Appl. Meteor., 20, n° 7, pp. 802-812, 1981.

Thonat et al. 2015: Thonat T., Crevoisier C., Scott N.A., Chédin A., Armante R. and Crépeau L., Signature of tropical fires in the diurnal cycle of tropospheric CO as seen from Metop-A/IASI, Atmos. Chem. Phys., *22, 13041-13057, 2015*, doi:10.5194/acp-15-13041-2015, 2015.

TRD GHG, 2017: Buchwitz, M., Aben, I., Anand, J., Armante, R., Boesch, H., Crevoisier, C., Detmers, R. G., Hasekamp, O. P., Reuter, M., Schneising-Weigel, O., Target Requirement Document, Copernicus Climate Change Service (C3S) project on satellite-derived Essential Climate Variable (ECV) Greenhouse Gases (CO_2 and CH_4) data products (project C3S_312a_Lot6), Version 1, 28-March-2017, pp. 52, 2017.

TRD GAD GHG, 2020: Buchwitz, M., Aben, I., Armante, R., Boesch, H., Crevoisier, C., Hasekamp, O. P., Wu, L.., Reuter, M., Schneising-Weigel, O., Target Requirement and Gap Analysis Document, Copernicus Climate Change Service (C3S) project on satellite-derived Essential Climate Variable (ECV) Greenhouse Gases (CO_2 and CH_4) data products (project C3S_312b_Lot2), Version 2.11, 9-April-2020, pp. 80, 2020.

Wofsy et al. 2012: Wofsy, S. C., Daube, B. C., Jimenez, R., et al.: HIPPO Merged 10-second Meteorology, Atmospheric Chemistry, Aerosol Data (R 20121129), Carbon Dioxide Information Analysis Center, Oak Ridge National Laboratory, Oak Ridge, Tennessee, USA, http://dx.doi.org/, 10.3334/CDIAC/hippo 010 (Release 29 November 2012), 2012.

Copernicus Climate Change Service

ECMWF - Shinfield Park, Reading RG2 9AX, UK

Contact: https://support.ecmwf.int/